

SYNTHESIS, CHARACTERISATION AND CORROSION INHIBITION SCREENING: Cu[EtBenzdte]₂ AND Cu[BuMedtc]₂

Nur Alia Atiqah Alias, Nabilah Syakirah Zolkifli, Mimi Wahidah Mohd Radzi, Nur Nadia Dzulkifli*

*School of Chemistry and Environment, Faculty of Applied Sciences
Universiti Teknologi MARA (UiTM), Cawangan Negeri Sembilan, Kampus Kuala Pilah, 72000 Kuala Pilah, Negeri Sembilan, Malaysia*

*Corresponding author: nurnadia@uitm.edu.my

Abstract

Mild steel plays an essential part in many construction industries due to its low cost and excellent mechanical properties. However, the use of strong acid in pickling, construction, and oil refining processes adds to a serious corrosion problem for mild steel. Two Cu(II) dithiocarbamate (DTC) complexes were successfully synthesised, namely Cu(II) ethyl-benzyl DTC (Cu[EtBenzdte]₂) and Cu(II) butyl-methyl DTC (Cu[BuMedtc]₂) complexes, by a condensation reaction and subsequently used to scrutinise the corrosion resistance activity towards mild steel in acidic media. The proposed structures of complexes were characterised by using the Fourier transform infrared (FTIR) and ultraviolet-visible (UV-Vis) spectroscopies. The melting point for Cu[EtBenzdte]₂ was found around 362–375°C, and 389–392°C for Cu[BuMedtc]₂. The percentages of Cu(II) found in Cu[EtBenzdte]₂ and Cu[BuMedtc]₂ were 7.6% and 7.5%, respectively. Both complexes were non-electrolyte based on the molar conductivity analysis. Their corrosion inhibition performances were tested by using a weight loss measurement. Cu[BuMedtc]₂ showed a good result as a corrosion inhibitor compared to Cu[EtBenzdte]₂. The complexes showed good effectiveness in sulfuric acid (H₂SO₄) compared to hydrochloric acid (HCl) solution. Furthermore, Cu[BuMedtc]₂ showed a good result as a corrosion inhibitor compared to Cu[EtBenzdte]₂ with the highest percentage of corrosion inhibition recorded at 91.8%. Meanwhile, the highest percentage of corrosion inhibition shown by Cu[EtBenzdte]₂ was only 86.9%. The lowest corrosion rate shown for Cu[BuMedtc]₂ was $8.1944 \times 10^{-4} \text{ cm}^{-1} \text{ h}^{-1}$. Meanwhile, the Cu[EtBenzdte]₂ showed the lowest corrosion rate only at $1.3194 \times 10^{-3} \text{ cm}^{-1} \text{ h}^{-1}$. This implies that Cu[BuMedtc]₂ showed lower corrosion rate but higher inhibition efficiency compared to Cu[EtBenzdte]₂.

Keywords: Dithiocarbamate, Corrosion, H₂SO₄, HCl

*Article History:- Received: 11 November 2020; Accepted: 17 February 2021; Published: 30 April 2021
© by Universiti Teknologi MARA, Cawangan Negeri Sembilan, 2021, e-ISSN: 2289-6368*

Introduction

Corrosion is one of the main issues in industries that causes environmental destruction and material property loss. Corrosion can be described as material destruction due to chemical reactions with the environment (Kruger and Begum, 2016). Due to their economic and safety implications, the corrosion issue has received significant attention. Most corrosion cases occur in industries due to exposure to acids, such as hydrochloric acid (HCl) and sulfuric acid (H₂SO₄) used during industrial acid cleaning. Various corrosion inhibitors are used to control and reduce the corrosion of metals in a corrosive medium in order to solve this problem. A chemical agent that could increase a metal resistance to corrosion is known as a corrosion inhibitor. Inhibitors could reduce the corrosion rate via several mechanisms. The main processes include reducing the reaction speed at anodic and cathodic sites, reducing the diffusion of ions to and from the metal surface, and improving the electrical resistance of the metal surface (Al-Amiery et al., 2014). The previous corrosion inhibitor widely used was a toxic inhibitor containing chromates and nitrites that could be synthesised at a cheaper cost (Ashassi-Sorkhabi et al., 2011). Corrosion inhibitors from chromate derivatives have also been reported to be carcinogenic and dangerous to the environment (Mohammadi et al., 2020). Furthermore, some organic compounds

had been recognised as environmentally friendly corrosion inhibitors, but their corrosion inhibition efficiency is very poor (Al-Rawashdeh et al., 2017). High solubility, strong, simple, inexpensive, and high inhibition efficiencies at a lower concentration are the criteria needed for a good corrosion inhibitor (Shetty, 2019). Efficient inhibitors are organic compounds that contain electronegative heteroatoms, including phosphorus (P), sulfur (S), nitrogen (N), and oxygen (O) in their structures, and have high electron density. The high electron density around all these atoms made them extremely basic and could withstand the corrosion effect (Elemike et al., 2017). Chelating compounds that could develop a chemisorbed film on the metal surface are considered the most efficient protection (Kicir et al., 2016). Dithiocarbamate (DTC) is suitable as an anti-corrosion agent due to the ease of creating self-assembled monolayers (SAMs) and high ability to bind with metals (Alshamaileh et al., 2014). In addition, DTC is a good corrosion inhibitor as it comprises more than one sulfur atom, which is more effective than nitrogen or oxygen atoms in donating electrons (Zhang et al., 2015). DTCs are classified as good metal chelating agents with high potential to donate electrons from the sulfur atom (-C = S- and -C-S-), and therefore, are highly compatible with many metals with d-orbital vacancies. A minimal number of studies had investigated the use of DTC compounds as corrosion inhibitors (Kicir et al., 2016). Furthermore, DTC compounds are often found to be more environmentally friendly and greener material as a biocompatible compound (Alshamaileh et al., 2014). In this study, two DTC complexes were synthesised by condensation, namely Cu(II) ethyl-benzyl DTC (Cu[EtBenzdte]₂) and Cu(II) butyl-methyl DTC (Cu[BuMedtc]₂) complexes. Cu[EtBenzdte]₂ complex was chosen as the inhibitor because of the presence of aromatic ring in their structure. The aromatic rings in some inhibitor compounds create a rich electron platform which promotes the adsorption of the compounds on the metal surface, thus, blocking the corrosion sites and preventing metal deterioration (Elemike et al., 2018). Meanwhile, Cu[BuMedtc]₂ complexes were chosen due to the presence of alkyl chain group. The inhibition efficiency would increase with the increase in alkyl chain length of the inhibitor which was due to the increase in the thickness of the protective layer formed (Shetty, 2019). DTC complexes were chosen as corrosion inhibitor compared to its ligand complexes, which would provide greater surface coverage due to the fact that the complexes would have a planar shape, hence, more binding capability with the metal (mild steel) surface. Inhibitor with a flat or horizontal geometry on the metal surface would cover a wider area compared to the same inhibitor with vertical or non-planar geometry inhibitor. Copper metal was chosen to bind with the ligand for copper is a noble metal that effectively resists corrosion. A recent study by Rbaa et al., (2020) indicated that Cu complexes showed better performance as inhibitor compared to Zn complexes because electronegativity of copper is greater than zinc. Cu complexes were also found to react more strongly with mild steel surface. Both complexes were characterised by using the Fourier transform infrared (FTIR) and ultraviolet-visible (UV-Vis) spectroscopies. The melting point for both complexes was recorded and the percentage of Cu(II) was studied by using gravimetric analysis. Molar conductivity measurement was also conducted on both complexes. Meanwhile, the corrosion inhibition of different inhibitor concentrations in H₂SO₄ and HCl, was determined by using the weight loss method.

Methods

Characterization

The infrared spectra were recorded on a Fourier Transform Infrared Attenuated Total Reflectance (FTIR-ATR), Perkin Elmer spectrophotometer model GX in the range of 4000–650 cm⁻¹. The electronic spectra were measured by a PG instrument T80/T80+ spectrophotometer in the range of 200–600 cm⁻¹ region for the starting materials and complexes with ethanol as a solvent. The characterisation was conducted by using a 1 cm quartz cuvette with a concentration of the solution of 1 × 10⁻⁵ M. The starting materials and complexes were subjected to melting point determination by using a melting point apparatus model SMP 10 Stuart and the measurement was taken into an open capillary tube. Meanwhile, molar conductivity measurements were performed at room temperature with a dimethylformamide (DMF) solvent by using the SI Analytic Lab 970 conductivity meter at 2 × 10⁻³ M concentration. Gravimetric analysis was done by using a furnace Model Lindberg/Blue.

Synthesis of Cu(II) dithiocarbamate complexes

$\text{Cu}[\text{EtBenzdtc}]_2$: The complex was synthesised at 1:1:1 ratio. An ethanolic solution of *N*-ethylbenzylamine (0.003 mol) was stirred for 30 min at 4°C before adding an ethanolic solution of carbon disulfide (0.003 mol). Ammonia was added dropwise to the mixture while stirring after 1 h. Thereafter, 0.003 mol of copper (II) chloride solution was added to the mixture. The product was filtered and washed with cold hexane after two hours of continuous stirring. The product was recrystallised by using acetonitrile and tetrahydrofuran (THF) using the 1:2 ratios, respectively. The product purity was checked by a thin-layer chromatography (TLC). The steps were repeated to synthesis $\text{Cu}[\text{BuMedtc}]_2$ with *N*-butylmethylamine as a starting material.

Corrosion Inhibition Study

Acidic solution of 1 M was prepared from 37% of HCl and 1 M of 95% H_2SO_4 by using the dilution method. The concentrations of the inhibitors in this study were 0.1 M, 0.01 M, and 0.001 M, which were prepared by diluting with 1 M HCl and H_2SO_4 . $2 \times 3.5 \text{ cm}^2$ of mild steel, which were cleaned by using emery paper and then washed with acetone and distilled water. The initial weight of the dried and cleaned mild steel was recorded. The mild steel was immersed in 1 M HCl without a corrosion inhibitor (i.e., synthesised complexes). Another specimen was immersed in 1 M HCl, but with the presence of different concentrations of inhibitors (i.e., 0.1 M, 0.01 M, and 0.001 M). All specimens were immersed for 24 hours and left to dry. The final weight of specimens was recorded and the corrosion inhibition activity was repeated by using H_2SO_4 .

Result and Discussion

Synthesis of $\text{Cu}[\text{BuMedtc}]_2$ and $\text{Cu}[\text{EtBenzdtc}]_2$

The complexes obtained were green precipitates, which were synthesised by the reaction of CuCl_2 with amine derivatives and carbon disulfide (CS_2) in a cold ethanol solution with the 1:1:1 ratio. Synthesis was carried out by using condensation method, or generally known as one-pot synthesis. The purpose of this method is to prepare DTC complexes through in situ synthesis. In this method, the usage of basic medium is important to conserve the amine (Odularu and Ajibade, 2019). The products were rinsed with a cold ethanol solution and dried in a desiccator. The melting points for $\text{Cu}[\text{EtBenzdtc}]_2$ were found around 362–375°C, and 389–392°C for $\text{Cu}[\text{BuMedtc}]_2$. Figures 1 and 2 show the proposed structures for both complexes of $\text{Cu}[\text{BuMedtc}]_2$ and $\text{Cu}[\text{EtBenzdtc}]_2$, respectively.

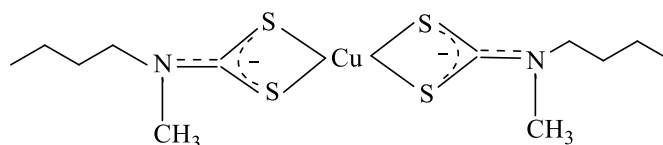


Figure 1. Proposed structure of $\text{Cu}[\text{BuMedtc}]_2$

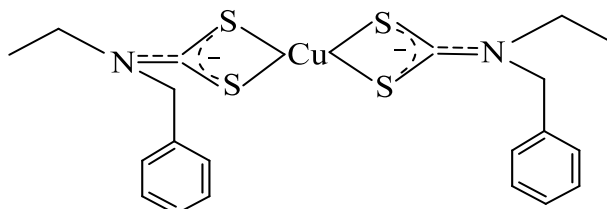


Figure 2. Proposed structure of $\text{Cu}[\text{EtBenzdtc}]_2$

Infrared Spectroscopy

Fourier transform infrared (FTIR) was used to determine the functional group present in the synthesised complexes, and it was also crucial in order to determine selected important vibration frequency for the synthesised complexes. Table 1 compiles the IR data obtained for Cu[BuMedtc]₂, Cu[EtBenzdte]₂, and their starting materials. Two significant stretching bands were observed for both complexes, which were $\nu(\text{C}=\text{N})$ and $\nu(\text{C}=\text{S})$. A new stretching band, known as $\nu(\text{C}=\text{N})$ or thioureide moiety, formed a partial bond due to the nitrogen atom that released the electrons into the sulphur atom through π -bond of thioureide moiety (Ziyaei et al., 2015) with the value of 1,537 cm⁻¹ for Cu[BuMedtc]₂ and 1,514 cm⁻¹ for Cu[EtBenzdte]₂. There was partial delocalisation of π -electron density within the DTC. The $\nu(\text{C}=\text{N})$ stretching band in both complexes showed a higher wavenumber compared to $\nu(\text{C}-\text{N})$ in *N*-ethylbenzylamine and *N*-butylmethylamine. This was due to the delocalisation of electrons towards the centre of the metal after being coordinated with DTC ligands. The 2^o $\nu(\text{N}-\text{H})$ band of amine derivatives was not present in the complexes' spectra, which proved the formation of thioureide moiety in the complexes (Awang et al., 2013). The stretching band of $\nu(\text{N}-\text{H})$ disappeared after the formation of metal complexes because of the hydrogen from amine had been deprotonated by ammonia (Latif et al., 2018). Stretching bands existed at 966 cm⁻¹ and 948 cm⁻¹ showed the $\nu(\text{C}=\text{S})$ reflected a bidentate-to-metal core coordination (Srinivasan, 2014). The $\nu(\text{C}=\text{S})$ in the complexes spectra shifted to the lower wavenumbers due to the decrease of the double bond character of $\nu(\text{C}=\text{S})$ in CS₂ (1,541 cm⁻¹) after complexation (Nqombolo and Ajibade, 2016).

Table 1. Summary of IR data for Cu[BuMedtc]₂ and Cu[EtBenzdte]₂ and their starting material

Compounds	Wavenumber (cm ⁻¹)					
	$\nu(\text{C}-\text{H})$	$\nu(\text{N}-\text{H})$	$\nu(\text{C}-\text{N})$	$\nu(\text{C}=\text{N})$	$\nu(\text{C}=\text{S})$	$\nu(\text{C}=\text{S})$
CS ₂	-	-	-	-	1541.0	-
<i>N</i> -butylmethylamine	2873.01	3408.73	1460.79	-	-	-
Cu[BuMedtc] ₂	2929.0	-	-	1537.25	-	966.72
<i>N</i> -ethylbenzylamine	2967.47	3369.04	1454.10	-	-	-
Cu[EtBenzdte] ₂	2936.5	-	-	1514.7	-	948.95

UV-Visible Spectroscopy

Table 2 displays the electronic transition spectral data of Cu[BuMedtc]₂ and Cu[EtBenzdte]₂. There was a transition of $\pi \rightarrow \pi^*$ at 237 nm, representing S-C=S in CS₂. Meanwhile, both complexes displayed an absorption peak at 270 nm, implying the $\pi \rightarrow \pi^*$ transition in N-C=S and S-C=S. The bathochromic shifting of the transition was due to the complexation effect (Ali et al., 2013). Furthermore, the $n \rightarrow \pi^*$ transition that overlaid at the shoulder peak of $\pi \rightarrow \pi^*$ for Cu[BuMedtc]₂ complex at 298 nm was described as the transition of electrons on the sulfur atom (Mamba et al., 2010). The ligand-to-metal charge-transfer (LMCT) transitions showed up at 430 nm (Cu[BuMedtc]₂) and 415 nm (Cu[EtBenzdte]₂), verifying the coordination of ligand to Cu(II) ion (Verma and Singh, 2015; Jeliakova et al., 2004). A weak absorption peak of more than 400 nm indicated the *d-d* transition due to the excitation of electrons in the *d*-metal orbitals (Nqombolo and Ajibade, 2016), deducing the presence of the coloured compounds.

Table 2. Electronic transition spectra data of Cu[BuMedtc]₂ and Cu[EtBenzdte]₂

Compounds	Transitions	λ_{max} (nm)
CS ₂	$\pi \rightarrow \pi^*$	237
Cu[BuMedtc] ₂	$\pi \rightarrow \pi^*$	270
	$n \rightarrow \pi^*$	298
	LMCT	430
	$d-d$	530
Cu[EtBenzdte] ₂	$\pi \rightarrow \pi^*$	270
	LMCT	415
	$d-d$	517

Molar Conductivity Measurement

This measurement showed that both Cu(II) complexes had low molar conductance values in the range between 0 and 30 Scm²mol⁻¹. This proved that both complexes were non-electrolyte in nature due to the low conductance values (Fazil and Minitha, 2020). Furthermore, the deduced data indicated that there were no counter ions present in the complexes. Non-electrolyte characteristic showed that the complex did not have any counter ion and indicated the ligand was directly bind to the metal centre (Latif et al., 2018).

Gravimetric Analysis

This analysis was conducted to identify the percentage of metal in the complexes (Pawar et al., 2013). The percentage of metal found in Cu[EtBenzdte]₂ and Cu[BuMedtc]₂ were 7.6% and 7.5%, respectively. The equations shown below are used to determine the percentage of metal in both complexes.

$$\text{Gravimetric factor (GF)} = \frac{\text{Molecular weight of analyte}}{\text{Molecular weight of precipitate}} \times \frac{a}{b}$$

$$\text{Weight of analyte} = \text{Weight of precipitate left} \times \text{GF}$$

$$\text{Percentage (\%)} \text{ of analyte} = \frac{\text{Weight of analyte}}{\text{Weight of precipitate}} \times 100\%$$

Calculation for Cu[EtBenzdte]₂ shown as below:

$$\frac{63.55}{484.223} \times \frac{2}{2} = 0.1312$$

$$0.0135 \times 0.1312 = 0.00177$$

$$\frac{0.00177}{0.0232} \times 100\% = 7.6\%$$

Meanwhile, calculation for Cu[BuMedtc]₂ shown as below:

$$\frac{63.55}{388.137} \times \frac{2}{2} = 0.1637$$

$$0.0129 \times 0.1637 = 0.00211$$

$$\frac{0.00211}{0.0281} \times 100\% = 7.5\%$$

Corrosion Inhibition Study

The anti-corrosion activity was carried out on mild steel in 1 M HCl and H₂SO₄ solution by using weight loss measurement. Weight loss measurement is one of the simplest technique to determine the corrosion rate on the metal in any medium of interest and weight loss will be recorded as a function of time (Oparaodu and Okpokwasili, 2014). The steel used in this study was mild steel with a chemical composition of C- 0.34%, Mn- 0.76%, P- 0.02%, Si- 0.3%, and the balance is Fe. The mild steels were submerged for 24 hours at room temperature in varying acid concentrations (i.e., 0.001 M, 0.01 M, and 0.1 M). Different concentrations were chosen to determine the effect of inhibitor's concentration towards corrosion rate and the lowest concentration, which was 0.001 M, was chosen to show the complexes was an effective corrosion inhibitor, even at low concentration. Cu[BuMedtc]₂ demonstrated a strong performance in the corrosion inhibition study compared to Cu[EtBenzdte]₂. This is most likely due to the presence of a shorter and less bulky alkyl substituent (-CH₃) in Cu[BuMedtc]₂, and hence, showing great anti-corrosion performance. Besides, the shorter the alkyl chain length in Cu[BuMedtc]₂, the higher the solubility of the complex in the acid medium (Shetty, 2019; Aiad and Negm, 2009). Meanwhile, the presence of a bulkier group in Cu[EtBenzdte]₂ caused steric hindrance, which affected the geometry or orientation of the inhibitor molecules on the metal surfaces and reduced their corrosion inhibition effectiveness (Blagus et al., 2010). Furthermore, both complexes demonstrated good corrosion inhibition effectiveness in H₂SO₄ compared to HCl solution. It could also be concluded that in this situation, chloride ions had more damaging effect than sulfate ions (Musa and Dzulkipli, 2018; Ajeel et al., 2012). In corrosive acidic environments, metallic surface becomes positive charged because of the accumulation of positive charges on the surface. Thereafter, the positively charged metallic surface attracts the counter ions of electrolytes, such as chloride ion. In acidic solution, organic inhibitors existed in their cationic forms, therefore, during the first stage of adsorption it negatively charged metallic surface and attracted positively charged inhibitor molecules by electrostatic interactions (physisorption) (Verma et al., 2019). Moreover, as the concentration of inhibitor complexes increased, the corrosion inhibition effectiveness also increased. Increasing inhibitor concentrations imply that more inhibitor molecules are adsorbed on the metal surface, providing greater surface coverage, and these compounds work as inhibitors by adsorption. Therefore, the risk of corrosion could be minimised (El-Lateef et al., 2015). Figures 3 and 4 present the anti-corrosion performance under different concentrations of inhibitors in HCl and H₂SO₄, respectively. The percentage of corrosion inhibition screening was calculated by using the equations below.

$$\Delta W = W_1 - W_2$$

$$CRW = \frac{W}{s \times t}$$

$$\theta = \frac{C^{\circ}RW - CRW}{C^{\circ}RW}$$

$$\% \eta_W = \frac{C^{\circ}RW - CRW}{C^{\circ}RW} \times 100\%$$

Where:

W_1 = the weight of mild steel before corrosion (g)

W_2 = the weight of mild steel after corrosion (g)

ΔW = the weight loss (g)

s = the surface area of the mild steel

t = the immersion time (h)

θ = surface coverage

C_{RW}° = the corrosion rate with the absence of inhibitor complex

C_{RW} = the corrosion rate with the presence of inhibitor complex

η_w = inhibitor efficiency

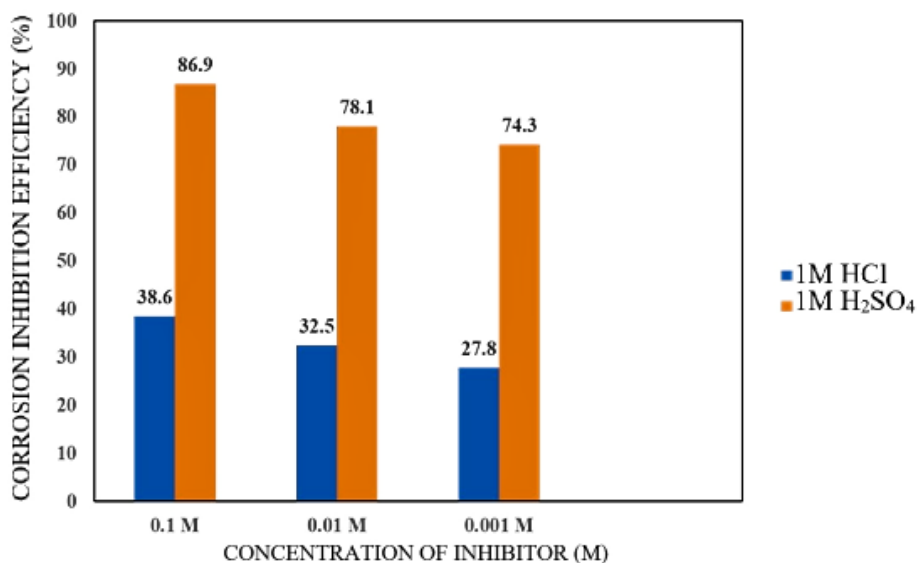


Figure 3. Inhibitor efficiency (%) versus concentration of inhibitor (M) in 1 M HCl and 1 M H₂SO₄ for Cu[EtBenzdte]₂

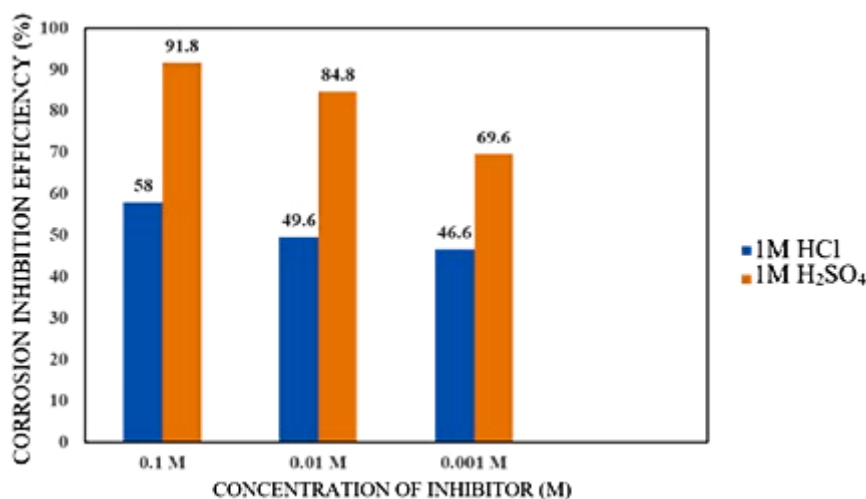


Figure 4. Inhibitor efficiency (%) versus concentration of inhibitor (M) in 1 M HCl and 1 M H₂SO₄ for Cu[BuMedtc]₂

Conclusion

Both Cu[EtBenzdte]₂ and Cu[BuMedtc]₂ were successfully synthesised and characterised by using FTIR and UV-Vis, melting point determination, gravimetric analysis, and molar conductivity measurement. Both complexes showed good corrosion inhibition effectiveness in H₂SO₄ compared to HCl with the highest inhibitor efficiency being recorded at 91.8%. Meanwhile, in the HCl medium, the highest efficiency recorded was only 58%. The complexes demonstrated promising anti-corrosion activity, whereby as the inhibitor concentration increased, the corrosion rate also decreased. The lowest corrosion rate was recorded when the highest concentration of inhibitor (0.1 M) was used. Overall, Cu[BuMedtc]₂ showed good performance as a corrosion inhibitor compared to Cu[EtBenzdte]₂ in both HCl and H₂SO₄ medium with the highest percentage recorded at 91.8% and 58%, respectively.

Acknowledgement

The authors would like to express their gratitude to the Faculty of Applied Sciences, Universiti Teknologi MARA, Negeri Sembilan Branch, Kuala Pilah Campus, Negeri Sembilan, Malaysia for providing the research facilities.

References

- Aiad, I., & Negm, N. A. (2009). Some Corrosion Inhibitors based on Schiff base Surfactants for Mild Steel Equipments. *Journal of Dispersion Science and Technology*, 30(8), 1142-1147.
- Ajeel, S., Mohammed Waadulah, H., & Abd Alkader Sultan, D. (2012). Effects of H₂SO₄ and HCl Concentration on the Corrosion Resistance of Protected Low Carbon Steel. *Al-Rafadain Engineering Journal*, 20(6), 70-76.
- Al-Amiery, A., Kadhum, A., Kadhum, A., Mohamad, A., How, C., & Junaedi, S. (2014). Inhibition of Mild Steel Corrosion in Sulfuric Acid Solution by New Schiff base. *Materials*, 7(2), 787-804.
- Ali, I., Wani, W. A., Saleem, K., & Hseih, M. (2013). Design and synthesis of thalidomide based dithiocarbamate Cu(II), Ni(II) and Ru(III) complexes as anticancer agents. *Polyhedron*, 56, 134–143.
- Al-Rawashdeh, N. A., Alshamsi, A. S., Hisaindee, S., Graham, J., & Al Shamisi, N. (2017). The Efficiency of Eco-Friendly Schiff bases as Corrosion Inhibitor for Stainless Steel in Hydrochloric Acid Solution. *International Journal of Electrochemical Science*, 12, 8535-8551.
- Alshamaileh, E., Kailani, M. H., Arar, S., & Al-Rawajfeh, A. E. (2014). Corrosion Inhibition of Aluminium by Cyclohexylamine Dithiocarbamate in Acidic Solution. *Studia Universitatis Babeş-Bolyai Chimia*, 59(3), 61-69.
- Ashassi-Sorkhabi, H., Asghari, E., & Ejbari, P. (2011). Electrochemical Studies of Adsorption and Inhibitive Performance of Basic Yellow 28 dye on Mild Steel Corrosion in Acid Solutions. *Acta Chimica Slovenica*, 58(2), 270-277.
- Awang, N., Baba, I., & Hamid, A. (2013). Synthesis, Characterization and Crystal Structure of Organotin (IV) *N*-Butyl-*N*-Phenyldithiocarbamate Compounds and Their Cytotoxicity in Human Leukimia Cell Lines. *Pakistan Journal of Biological Sciences*, 16(1), 12-21.
- Blagus, A., Cinčić, D., Friščić, T., Kaitner, B., & Stilinović, V. (2010). Schiff bases Derived from Hydroxyarylaldehydes: Molecular and Crystal Structure, Tautomerism, Quinoid effect, Coordination compounds. *Macedonian Journal of Chemistry and Chemical Engineering*, 29(2), 117.
- Elemike, E. E., Nwankwo, H. U., & Onwudiwe, D. C. (2018). Synthesis and characterization of Schiff bases NBBA, MNBA and CNBA. *Heliyon*, 4(7), 1-25.
- Elemike, E. E., Onwudiwe, D. C., Nwankwo, H. U., & Hosten, E. C. (2017). Synthesis, Crystal structure, Electrochemical and Anti-Corrosion Studies of Schiff base Derived from *o*-toluidine and *o*-chlorobenzaldehyde. *Journal of Molecular Structure*, 1136, 253-262.
- El-Lateef, H. M., Abu-Dief, A. M., & El-Gendy, B. E. D. M. (2015). Investigation of Adsorption and Inhibition Effects of Some Novel Anil Compounds towards Mild Steel in H₂SO₄ Solution: Electrochemical and Theoretical Quantum Studies. *Journal of Electroanalytical Chemistry*, 758, 135-147.

Fazil, S., & Minitha, R. (2020). Studies of some dioxo molybdenum(VI) complexes of a polydentate ligand. *Materials Today: Proceedings*.

Jeliazkova, B., Dimitrova, A., & Doicheva, M. (2004). Charge-transfer photolysis of copper(II) dithiocarbamate mixed-ligand complexes in toluene/alcohol solutions. *Spectrochimica Acta Part A: Molecular and Biomolecular Spectroscopy*, 60(6), 1291-1297.

Kıcır, N., Tansug, G., Erbil, M., & Tuken, T. (2016). Investigation of ammonium (2, 4-dimethylphenyl)-dithiocarbamate as a new, effective corrosion inhibitor for mild steel. *Corrosion Science*, 105, 88-99.

Kruger, J., & Begum, S. (2016). Corrosion of Metals: Overview, *In Reference Module in Materials Science and Materials Engineering*. Elsevier Inc.

Latif, N. S. H., Ghazali, S. A. I. S. M., Abdullah, E. N., Lahuri, A. H., Ngatiman, M. F., & Dzulkifli, N. N. (2018). Synthesis, Structural, Density Functional Theory, and X-Ray Diffraction Study of Zn(II) *N*-Isopropylbenzylthiocarbamate: Anti-Corrosion Screening in Acid Media. *Indonesian Journal of Chemistry*, 18(4), 755-765.

Mamba, S. M., Mishra, A. K., Mamba, B. B., Njobeh, P. B., Dutton, M. F., & Fosso-Kankeu, E. (2010). Spectral, thermal and in vitro antimicrobial studies of cyclohexylamine-*N*-dithiocarbamate transition metal complexes. *Spectrochimica Acta Part A: Molecular and Biomolecular Spectroscopy*, 77(3), 579-587.

Mohammadi, I., Shahrabi, T., Mahdavian, M., & Izadi, M. (2020). cerium/diethylthiocarbamate complex as a novel corrosion inhibitive pigment for AA2024-T3. *Scientific Reports*, 10, 1-15.

Musa, S. A., & Dzulkifli, N. N., (2018). [Zn(TAC)]Cl complex Potential as Corrosion Inhibitors: Synthesization and Characterization. *Journal of Academia*, 6(2), 12-17.

Nqombolo, A., & Ajibade, P. A. (2016). Synthesis and spectral studies of Ni(II) dithiocarbamate complexes and their use as precursors for nickel sulphides nanocrystals. *Journal of Chemistry*, 2016, 1-10.

Odularu, A. T., & Ajibade, P. A. (2019). Dithiocarbamates: challenges, control, and approaches to excellent yield, characterization, and their biological applications. *Bioinorganic chemistry and applications*, 2019, 1-16.

Oparaodu, K. O., & Okpokwasili, G. C. (2014). Comparison of percentage weight loss and corrosion rate trends in different metal coupons from two soil environments. *International Journal of Environmental Bioremediation and Biodegradation*, 2(5), 243-249.

Pawar, J. R. G. N. S., Bendre, R. S., College, P., & Amalner, M. S. (2013). Synthesis, spectral and biological study of four and five coordinate copper(II) complexes derived from 5-chloro-2-hydroxyacetophenone-*N*-(4)-methyl thiosemicarbazone. *School of Chemical Science, NMU*, 5(2), 111–117.

Rbaa, M., Benhiba, F., Galai, M., Abousalem, A. S., Ouakki, M., Lai, C. H., Lakhri, B., Jama, C., Warad, I., Ebn Touhami, M., & Zarrouk, A. (2020). Synthesis and characterization of novel Cu(II) and Zn(II) complexes of 5-[[2-Hydroxyethyl] sulfanyl] methyl}-8-hydroxyquinoline as effective acid corrosion inhibitor by experimental and computational testings. *Chemical Physics Letters*, 754, 137771-137784.

Shetty, P. (2019). Schiff bases: An Overview of Their Corrosion Inhibition Activity in Acid Media against Mild Steel. *Chemical Engineering Communications*, 1-45.

Srinivasan, N. (2014). Superlattices and Microstructures Synthesis and characterization of functionalized dithiocarbamates: New single-source precursors for CdS. *Superlattices and Microstructures*, 65, 227–239.

Verma, C., Haque, J., Quraishi, M. A., & Ebenso, E. E. (2019). Aqueous phase environmental friendly organic corrosion inhibitors derived from one step multicomponent reactions: A review. *Journal of Molecular Liquids*, 275, 18-40.

Verma, S. K., & Singh, V. K. (2015). Synthesis and characterization of ferrocene functionalized transition metal dithiocarbamate complexes: Investigations of antimicrobial, electrochemical properties and a new polymorphic form of [Cu{K₂S₂S₂CN(CH₂C₄H₉O)CH₂Fc}₂]. *Journal of Organometallic Chemistry*, 791, 214-224.

Zhang, X. H., Liao, Q. Q., Nie, K. B., Zhao, L. L., Yang, D., Yue, Z. W., Ge, H. H., & Li, Y. J. (2015). Self-assembled monolayers formed by ammonium pyrrolidine dithiocarbamate on copper surfaces in sodium chloride solution. *Corrosion Science*, *93*, 201-210.

Ziyaci, A., Torabi, S., Amani, V., Notash, B., & Reza, M. (2015). Synthesis and characterization of metal dithiocarbamate derivatives of 3-((pyridin-2-yl) methylamino)propanenitrile. *Polyhedron*, *102*, 643–648.